Multiscale techniques for 3D imaging of magnetic data for archaeo-geophysical investigations in the Middle East

Florio, Giovanni; Cella, Federico; Speranza, Luca; Castaldo, Raffaele; Pierobon Benoit, Raffaella; Palermo, Rocco

IMPORTANT NOTE: You are advised to consult the publisher's version (publisher's PDF) if you wish to cite from it. Please check the document version below.

Document Version
Publisher's PDF, also known as Version of record

RESEARCH ARTICLE

Multiscale techniques for 3D imaging of magnetic data for archaeo-geophysical investigations in the Middle East: the case of Tell Barri (Syria)

Giovanni Florio[1] | Federico Cella[2] | Luca Speranza[3] | Raffaele Castaldo[4] |
Raffaella Pierobon Benoit[5] | Rocco Palermo[6]

[1]Dipartimento di Scienze della Terra, dell'Ambiente e delle Risorse, Università degli Studi «Federico II», Naples, Italy

[2]Dipartimento di Biologia, Ecologia e Scienze della Terra, Università della Calabria, Rende, Italy

[3]Edison S.p.A., Exploration & Production Division, Edison, Milan, Italy

[4]Consiglio Nazionale delle Ricerche (CNR), Istituto per il Rilevamento Elettromagnetico dell'Ambiente (IREA), Naples, Italy

[5]Dipartimento di Studi Umanistici, Università degli Studi «Federico II», Naples, Italy

[6]Institute of Archaeology, University of Groningen, Groningen, The Netherlands

Correspondence
Federico Cella, Università della Calabria, Dipartimento di Biologia, Ecologia e Scienze della Terra.. Rende (CS), Italy.
Email: federico.cella@unical.it

Abstract

Recent techniques of three-dimensional (3D) imaging of potential field anomalies are effective in estimating the source position in the subsurface by exploiting both the differentiation of the field and the stability of the method. Such a processing is fast and especially suitable for detecting isolated and compact sources, as usually are those of archaeological interest. Among these methods we employed techniques that take advantage from innovative concepts like the multiscale transformation and the scaling function, going well beyond the standard procedures usually employed for data processing with archaeological purposes. We interpreted magnetic data acquired during two geophysical surveys carried out in 2008 and 2010 at Tell Barri, in north-eastern Syria. Tell Barri is a relevant site for the history of North Mesopotamia. The earliest settlement dates back to the end of the fourth millennium BCE whereas the site has been occupied – with no major breaks – until the fourteenth century CE. Based on the magnetic data interpretation, we have selected a test area as a target for an archeological excavation. The excavation found ancient structures closely matching the magnetic source revealed by the geophysical imaging. Since both the ground soil and the material of buried archaeological structures are representative of several ancient settlements in a much larger area (Upper Mesopotamia), we believe that such a geophysical approach could be successful in many archaeological sites scattered through this broad region.

KEYWORDS

3D imaging, applied geophysics, archaeogeophysics, magnetic methods, multi-scale analysis, Syria, tell Barri

1 | INTRODUCTION

Tell Barri is an archeological settlement in north-eastern Syria in the Al-Hasakah Governorate (Figure 1(a)). It lays along the eastern bank of the wadi (seasonal stream) Jaghjagh, a small tributary of the Khabur River, and hence sub-tributary of the Euphrates. The most noticeable element of this site, from the morphological and archeological point of view, is the 'tell' (Figure 1(b)) outcropping just north of the Italian Archaeological Mission (36°44′11.3″N; 41°7′34.5″E). A *tell* (Arabic = hill) is an artificial mound that is largely widespread in the Eastern Mediterranean region and the Near East. It is formed by the gradual accumulation of occupational and building debris over the millennia (Figure 2). The settlements are largely the product of an architectural tradition that relies on sun-dried mud bricks as primary
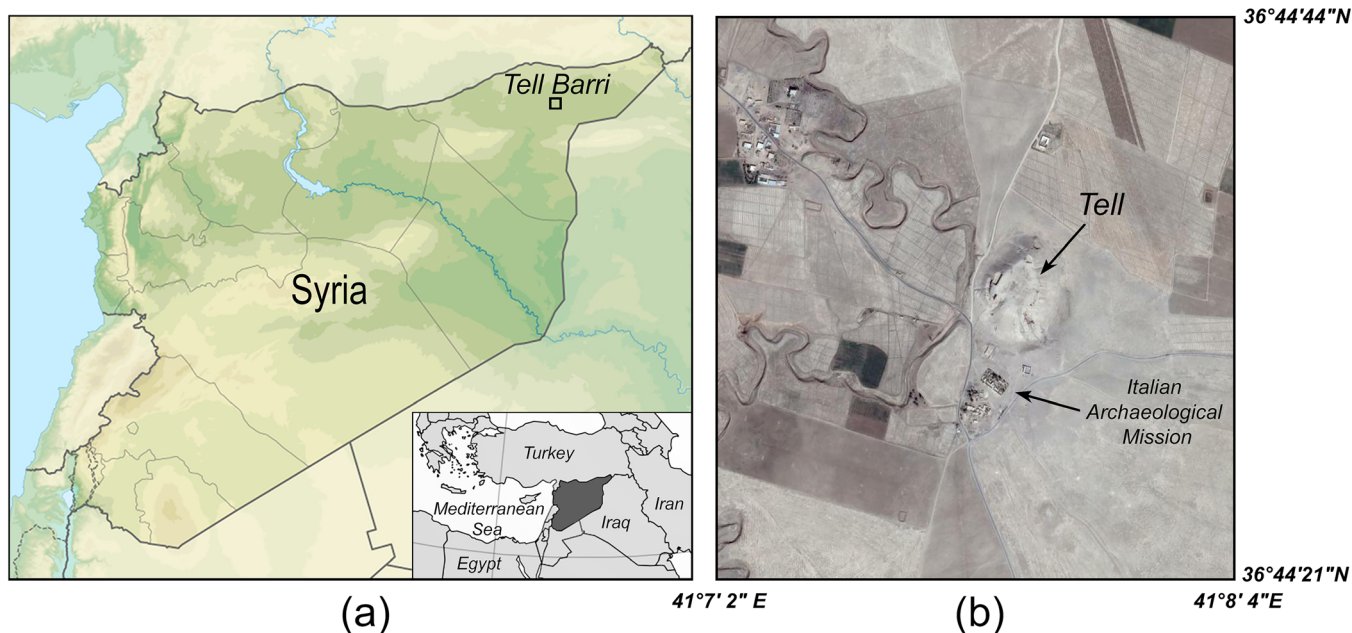
FIGURE 1 (a) Geographical map of Syria showing, in its north-eastern sector, the position of the Tell Barri site (black square); (b) satellite image of the area (black square in (a)) [Colour figure can be viewed at wileyonlinelibrary.com]
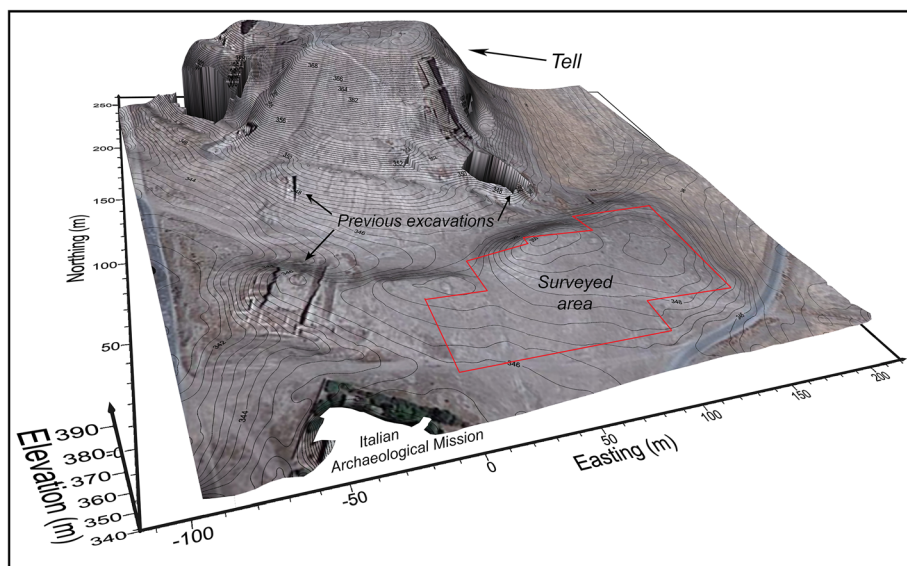

FIGURE 2 Satellite image and digital elevation model of the Tell Barri area (contour lines each 0.4 m). The red line encloses the geophysical survey area. The reference point with local coordinates 0,0 (south-western edge of the survey area) has geographic coordinates: Longitude 41°7′35.95″E, Latitude 36°44′12.26″N [Colour figure can be viewed at wileyonlinelibrary.com]

building material; as mud-brick buildings deteriorated, they were levelled and new structures were built over them. Such architectural tradition is still in use in rural areas of Syria, Iraq and south-eastern Turkey.

The site of Tell Barri was inhabited for a long period, with no major breakages in the occupational history – from the fourth millennium BCE until the middle Islamic period (fourteenth century CE; Pecorella, 1998; Pierobon Benoit & Pecorella, 2008; Pierobon Benoit, 2018; Palermo, 2019).

A sacred complex with shrines, courtyards, service buildings and a conspicuous quantity of votive objects (first half of third millennium BCE) testifies that the site had a complex administrative organization. The settlement was of regional importance during the second

millennium BCE. Tell Barri site was then known as Kahat, famous for the temple of the storm God, recorded in written texts. Traces of a large palatial building dated to the period of Adad-Nirari I (ca 1300 BCE), and rich elite tombs testify the importance of Tell Barri in this period. The western part of the acropolis was occupied, by another palatial residence, possibly connected to the Assyrian king Tukulti-Ninurta II (early ninth century BCE). Limited, but significant evidence, confirms that the site was not abandoned after the fall of the Assyrian Empire at the very end of the seventh century BCE, and in fact domestic structures and small working areas have been securely dated to the Achaemenid period (sixth–fourth century BCE). Tell Barri seems to remain a site of minor importance also in the Hellenistic period (late fourth–late second century BCE). A production area possibly connected

to dying activities has been excavated on the south-western slope of the mound and scattered Hellenistic period ceramics have been unearthed in the disturbed contexts all over the mound. Between the late first century BCE and the early third century CE (Parthian–Roman period) Tell Barri experiences a phase of major urbanization. Excavation data certainly proves that it regained a regional importance. The acropolis is now walled with a complex defensive system (Great Circuit Wall) with gates, towers and double curtains areas. The structure was built with a lower part in evenly organized fired bricks and the upper part – now completely lost – possibly in mudbricks. Dating evidence suggests that this monumental work was erected between the first century BCE and the first century CE, and destroyed – most likely by a violent event – at the beginning of the second century CE. The settlement, in this phase, occupied the entire acropolis (with later evidence of private dwellings, storage rooms and small production areas to the west) and the lower town, where an architecturally articulated large building was erected close to the Jaghjagh southwest of the tell. In this period Tell Barri is inserted in a wide network of trade and contacts with both East and West. Evidence of Roman period material culture (coins, distinctive Roman pottery, and a fragment of Latin inscription) testify the interest of Rome for the site and the area in general, which constituted the easternmost limit of the Empire.

During the Late Antiquity (fourth–seventh century CE) the site continues to be occupied as testified by new buildings and artefacts that show Tell Barri as a site inserted in regional and trans-regional contacts, despite the troubled political scenario of the sixth and early seventh century CE.

The life on the *tell* continues until the fourteenth century CE. From the architectural and material culture evidences of two major phases of occupation can be discerned. Excavation data have shown a series of transformation in the lower town dated to the early Islamic period, possibly connected to agricultural intensification processes. In the later phase, domestic structures and household-related production areas have been excavated on the acropolis.

The excavation of the site started in 1980 under the direction of Paolo Emilio Pecorella and continued until 2010 (R. Pierobon Benoit director) when the Italian Archaeological Mission was forced to a halt by the troubled events that have interested Syria since then. Artefacts from Tell Barri, including cuneiform tablets, are exposed in the museums of Aleppo and Deir Ez-Zor, in Syria.

In recent times, the interest was mainly targeted toward the area located just south of the *tell* in order to investigate the extension of the lower town. Indeed, previous excavations in this area revealed elements of a domestic complex of the Parthian period (ca 100 BC–
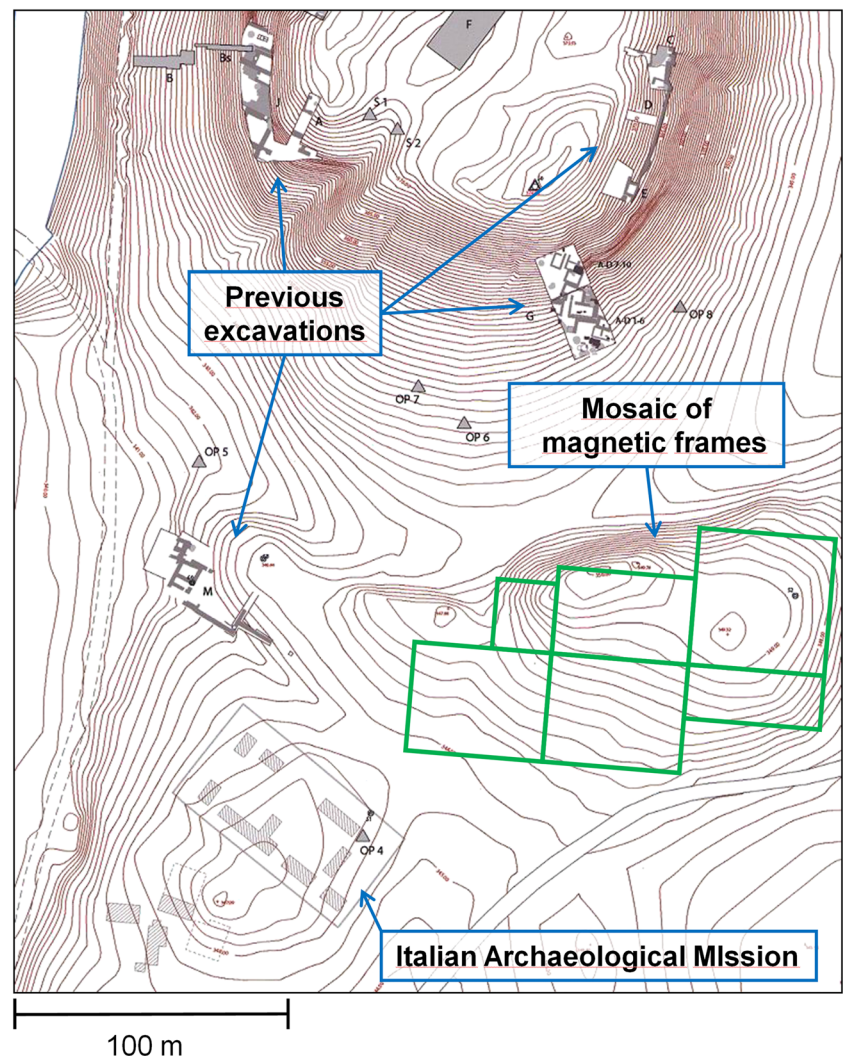

FIGURE 3 Topographic map of the archaeological site. The green boxes indicate the sectors of variable size and shape in which the surveyed area was divided [Colour figure can be viewed at wileyonlinelibrary.com]

200 AD), presumably houses and production areas. A recent acquisition of an U2 declassified image of Tell Barri (courtesy of Jason Ur, Harvard University, Cambridge, MA, USA) has shown how the lower town of the site was much more extended than previously thought. Anthropic soils and possible buried architectural features are visible in the north and to a larger extent to the east of the main mound. However, given the large extent of this area, a geophysical prospection that covered the whole lower town was prohibitive. The Tell Barri team decided thus to focus on specific zones in the immediate proximity of the main mound in order to investigate the direct relation with the settlement on the acropolis and the extended areas to the south.

1.1 | Magnetic method

The results provided by a large number of surveys carried out in the last years confirmed magnetic prospecting as one of the most performing and effective geophysical techniques for the exploration of archaeological sites (e.g. Gaffney, 2008; Fedi, Cella, Florio, La Manna, & Paoletti, 2017, and references cited therein). Its soundness is due to the existence of a contrast in magnetic properties between the cover soil and most archeological buried structures. This contrast generates magnetic anomalies with amplitudes ranging from a few or tenths of nanotesla in the case of floorings, graves and dwelling walls, to hundreds of nanotesla for 'fired' structures (pottery, kilns, hearths and crockery) and up to some thousands of nanotesla in the presence of buried ferrous objects like tools, slag or weapons (Gibson, 1986; Larson, Lipo, & Ambos, 2003, and references cited therein). A significant advantage is often given by the measure of the vertical gradient of the magnetic field, using a double sensor system (e.g. Breiner, 1973). This allows increasing the spatial resolution of the measured anomalies and obtaining measurements independent from the diurnal variations of the Earth's magnetic field and from regional background fields. In addition, since the vertical gradient of the magnetic field decays with the fourth power of the distance to the source, the anomalies generated by sources of archaeological interest, usually buried at shallow depths, are enhanced with respect to the deeper ones, often associated to a geologic origin.

Tell Barri, as of many other similar sites within the Tigris-Euphrates Basin, does not represent an easy task for geophysical prospecting targeted to the archeological investigation. This is due to the
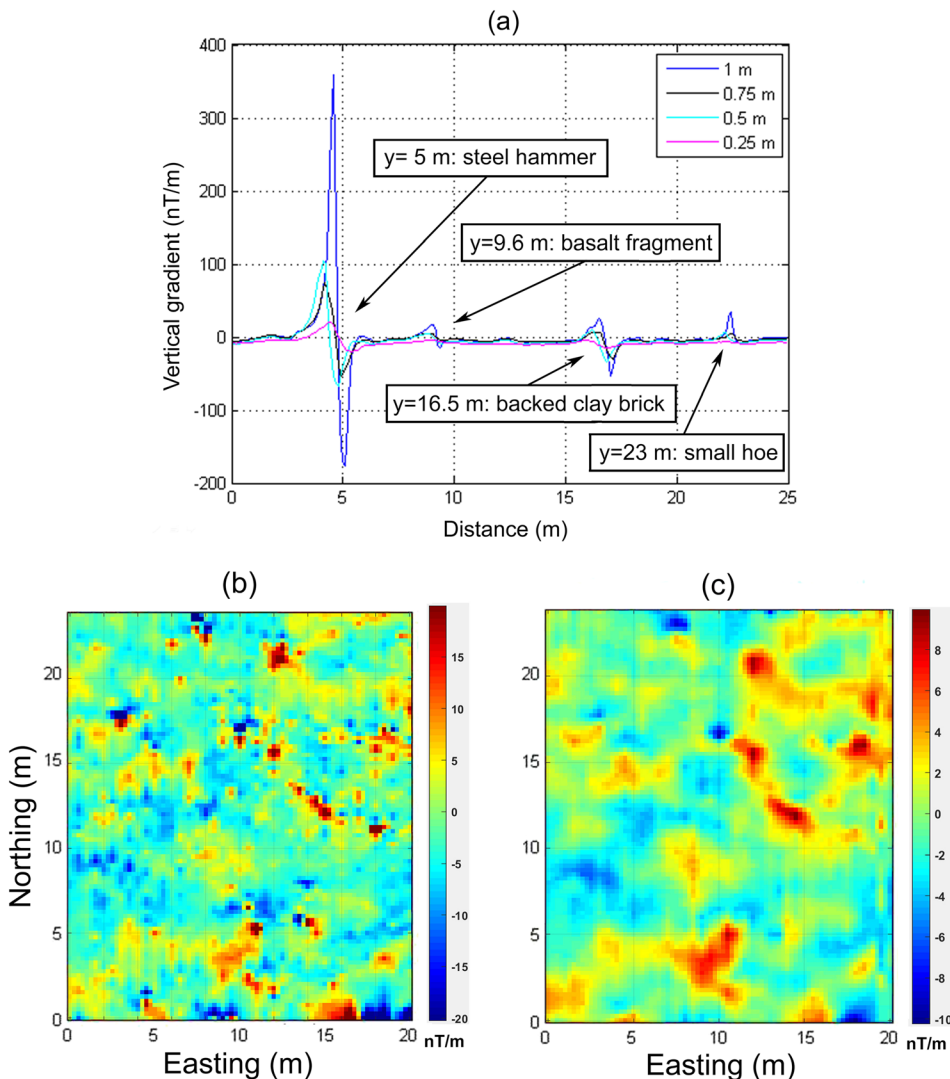
FIGURE 4 Tests for setting the best magnetic gradiometer configuration. (a) Magnetic vertical gradient measured along a test profile by varying the distance between the sensors (100 cm, 75 cm, 50 cm, and 25 cm). In these tests the average heights above the ground level was also varied (95 cm, 102.5 cm, 95 cm, and 132.5 cm, respectively). The arrows indicate the position of four small, highly magnetized sources placed on the ground and the related dipolar anomalies. (b, c) Maps of the vertical gradient measured north of Area 3 (Figure 7) by using (b) the standard gradiometric configuration (distance between sensors = 1 m; height above the ground = 95 cm) and (c) the chosen configuration (distance between sensors = 0.25 m; height above the ground = 132.5 cm) [Colour figure can be viewed at wileyonlinelibrary.com]

building techniques traditionally used in this region over thousands of years until now, combined with the geological features of the outcropping deposits. These consist mostly of alluvial and lacustrine fine sediments, aged from Pliocene to the present (Ilaiwi, 1985), containing a high fraction of dry siltous-clay particles. Such a material favoured the formation at the surface of young soils (medium to fine) with weathered levels, supporting the hypothesis of a ground soil with low susceptibility around Tell Barri area. Unfortunately, these sediments are the only building material available over a broad area and were used since the third millennium BCE and until now in the manufacture of sun-dried mudbricks, the main building blocks for houses and other structures. These conditions should imply a very weak susceptibility contrast between buried materials and surrounding ground. Nevertheless, settlements (mostly dated to the Parthian, Sassanian and Islamic period) built with highly susceptive baked-clay bricks are known to be present in the study area. This made us confident that the magnetic prospecting can be a useful geophysical prospecting.

1.2 | Survey layouts

The geophysical investigation at Tell Barri was carried out during two different surveys on September 2008 and September 2010 over an almost flat area of about 10 750 m^2 and 15 250 m^2, respectively, at

elevations ranging from 340 to 350 m above sea level (a.s.l.) (Figure 3). The surveyed area involved six sectors of variable size and shape.

We used an alkali vapour GEM GSMP40G potassium magnetometer, in vertical gradiometric configuration. This magnetometer has a very high resolution (0.009 nT at ten samples per second) and acquisition rate (up to 20 Hz). The magnetic measurements were acquired with sampling rates of 20 measures per second, corresponding to an inline sampling step of about 0.15 m along north–south oriented equidistant profiles spaced 0.5 m. The geographic positioning of the geophysical maps was ensured by georeferencing all the measurements by differential global positioning system (GPS) (Leica System 500).

Since the first measurements, it was clear that the magnetic data were affected by a low signal-to-noise (S/N) ratio. This was due to the presence of a large number of small, highly magnetic sources scattered on the ground surface and consisting of empty cans, baked brick fragments and variously sized basaltic stones. Despite the efforts to remove the visible objects from the surveyed area, the low quality of results persisted because of the presence of many other small noise sources hidden just below the topsoil.

The problem was tackled by modifying the standard GSMP40 geometry of the double sensor system, varying the distance between
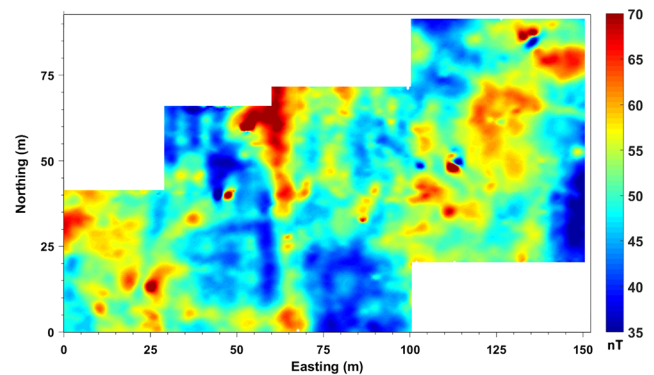
FIGURE 6 Map of the total magnetic field anomalies in the surveyed area after the data processing described in section entitled 'Magnetic data processing' [Colour figure can be viewed at wileyonlinelibrary.com]
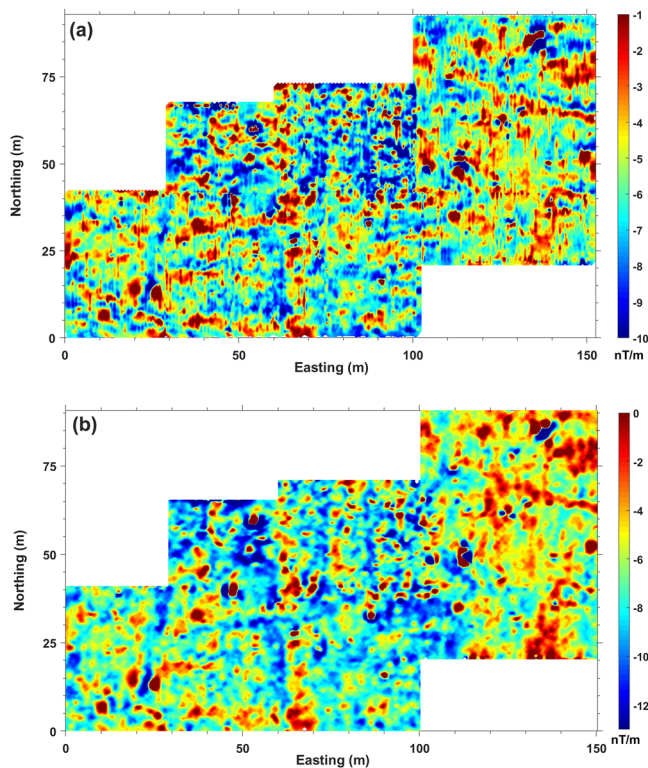

FIGURE 5 Map of the vertical gradient of the total magnetic field in the surveyed area (a) before and (b) after the data processing described in section entitled 'Magnetic data processing'. The plotting range of the magnetic gradient values was arbitrarily reduced to improve the visualization [Colour figure can be viewed at wileyonlinelibrary.com]

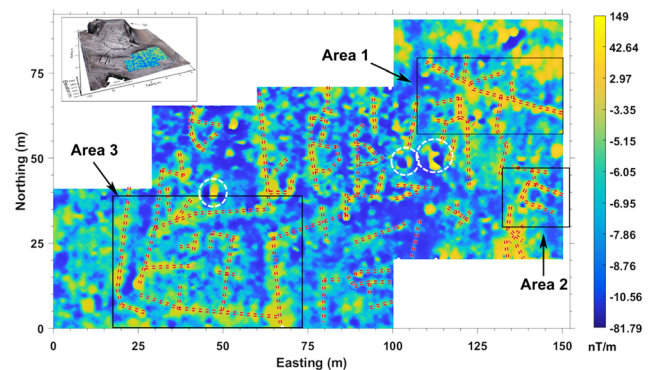**FIGURE 7** Map of the vertical gradient of the total magnetic field in the surveyed area after data processing and reduction to the pole. Red dashed lines highlight the most significant patterns of anomalies. Black rectangles indicate the location of three areas investigated in detail. White dashed circles highlight some high-amplitude anomalies [Colour figure can be viewed at wileyonlinelibrary.com]

the two sensors as well as their average altitude above the ground. In other words, we tried to obtain a different setup of the gradiometer aimed at minimizing the effects of near surface highly magnetized sources. A session test was carried out on site along a profile, by placing on the ground several objects (a basalt stone having the average size of those found within the area, a steel hammer, some baked bricks and a small metallic hoe). We measured the vertical gradient of the magnetic field repeatedly along such a profile, varying the geometry of the sensors in four different gradiometric configurations. The distance between the two sensors was set at 100 cm (standard distance for this instrument), 75 cm, 50 cm and 25 cm, with the gradiometer midpoint located at 95 cm, 102.5 cm, 95 cm and 132.5 cm, respectively (elevations from ground resulting from the operator's height).
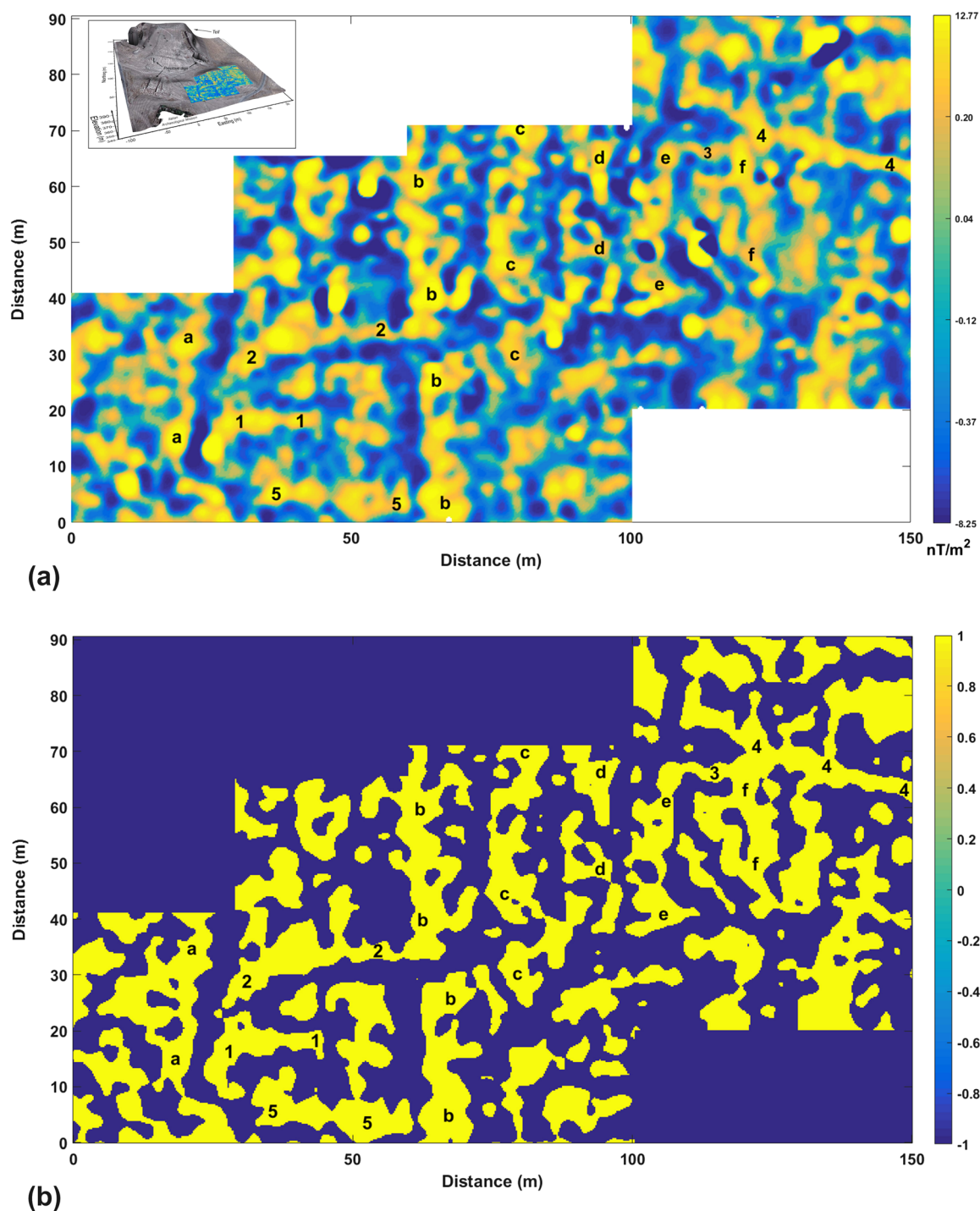

FIGURE 8 Analysis of the magnetic gradient anomalies. (a) Map of the vertical derivative of the measured vertical gradient of the magnetic field upward continued to 1.5 m; (b) signum transform of (a). Letters and numbers indicate the main linear anomaly trends in a south–north or west–east directions, respectively [Colour figure can be viewed at wileyonlinelibrary.com]

Despite the unusual geometry, the last configuration (distance between sensors of 25 cm and midpoint at 132.5 cm from the ground) assured the best results, with the attenuation of the strong magnetic field generated by shallow, highly magnetized, objects (Figure 4(a)). In fact, because of the greater distance of the system from the ground level, the signal due to shallow objects strongly reduces its amplitude and the weak anomalies due to deeper sources of possible archeological interest results are relatively enhanced. This effect is emphasized by the short distance between the sensors. A clear example of the advantages given by adopting the new gradiometer configuration can be appreciated in Figure 4 by comparing the maps of the vertical gradient surveyed in the same test area (located north of Area 3 in Figure 7) with the standard gradiometric configuration (Figure 4(b)) and the chosen one (Figure 4(c)). It is evident that cleaner and more continuous trends of anomalies are obtained when using the new gradiometer setting. Notice that in the first case the gradient anomalies have a stronger amplitude than when the modified configuration is used, due to both the greater sensor separation (1 m vs 0.25 m) and the lower distance to the ground (0.95 m vs 1.32 m). Moreover, the small distance between sensors improves the quality of the measured vertical gradient. In fact, in theory, to measure an accurate vertical gradient the distance between the two sensors should be very small with respect to the distance to the magnetized source (e.g. Breiner, 1973).

1.3 | Magnetic data processing

Despite the special gradiometer configuration used, the data still shows the presence of strong signals that probably obscure many anomalies with archaeological meaning, but with lower amplitude. Thus, data were processed by employing a despiking procedure based on median filters (Tabbagh, 1999) and were plotted using a histogram equalization algorithm, able to image the data with the same emphasis for signals with both low and high amplitudes.

Moreover, the maps appeared affected also by another typical linear noise due to the geometry of the data acquisition procedures; this 'displacement error' (or 'heading error') is caused by the different position occupied by the instrument-operator system when it runs along adjacent lines moving in opposite directions. The problem was partially solved by computing the difference between the mean values of odd and even lines. The result was used to equalize the mean values of the measured field of both sets of lines (Ciminale & Loddo, 2001). A more serious problem was instead caused by the irregular lag existing between adjacent profiles and producing a 'zigzag' effect along the edges of the anomalies. Such a noise was reduced by using a statistical method based on the cross-correlation among adjacent data profiles (Ciminale & Loddo, 2001).

When data surveyed on single sub-areas are combined to provide a complete map, the possible presence, in the adjoining datasets, of different trends, offsets or interference effects often causes the occurrence of fictitious anomalies along the boundary zones. Such a problem was solved through additional processing steps (grid stitching) using the 'GridKnit' tool included in the Geosoft ™ software. First, the

mean value among the sub-areas is adjusted by constant values to minimize the differences at the boundaries. Second, the measured values in a belt at the boundaries of the single sub-areas are corrected to guarantee a smooth transition from one to another, and third, the data are merged by an interpolation of the modified dataset.

However, the techniques mentioned earlier did not completely suppress a residual noise in the direction parallel to the measurement lines, shaped as stripes elongated in a north–south direction. To remove this noise, a directional filtering based on the discrete wavelet transform (DWT) was applied (Fedi & Quarta, 1998), allowing a complete 'decorrugation' of the magnetic grid. This kind of filtering allows a localized and sharp removal of the directional noise, providing better results than filters based on other basis functions (i.e. cosine filtering in the Fourier domain). The quality of this filtering was assessed by a careful inspection of the filtered signal map, checking that no distortion of the main anomaly trends is produced, and of the residual signal map, where only north–south stripes should be present, uncorrelated with the useful signal (for more details on this filtering see Appendix A).

As a last step, to improve the visual interpretation of the dipolar magnetic anomalies, a reduction to the pole procedure (e.g.Baranov,

(a)

(b)
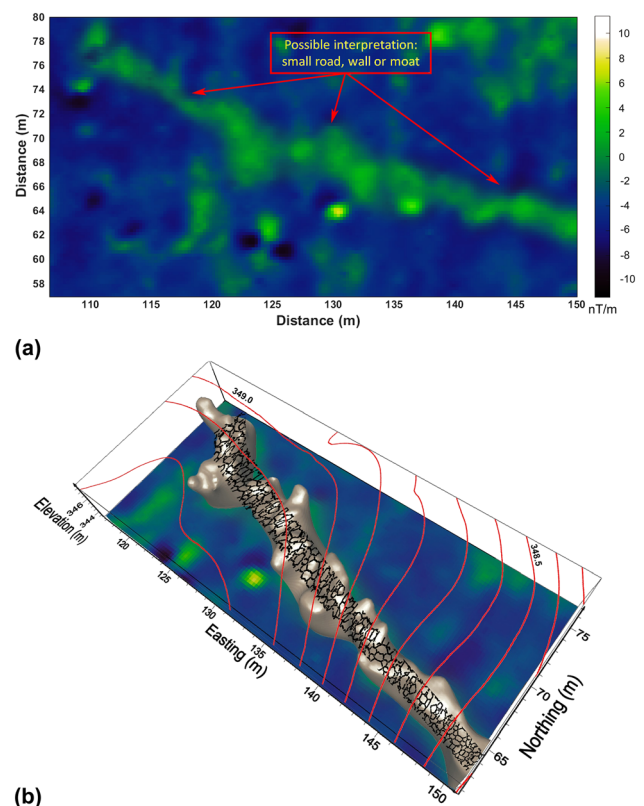
FIGURE 9 Data interpretation in Area 1 (for the location, see Figure 7). (a) Magnetic vertical gradient field, showing a linear anomaly in west-northwest–east-southeast direction, possibly interpretable a small road or moat; (b, c) iso-surface representation of the source imaging obtained by depth from extreme points (DEXP) method. The source centre is identified at a depth ranging from 0.7 m to 1.1 m below the ground level. The topography is indicated with red contours each 0.1 m. The magnetic vertical gradient is shown for reference in the background [Colour figure can be viewed at wileyonlinelibrary.com]

1975 ; Blakely, 1996) was employed by assuming a magnetization direction parallel to that of the Earth's magnetic field in the investigated area (declination: −14°35′; inclination: 54°36′). The reduction to the pole (see also Appendix A) transforms the measured magnetic anomalies in those that would be observed if the same sources had a vertical magnetization and were at the magnetic pole. Consequently, in a reduced to the pole magnetic map the magnetic sources should result in locations just in correspondence with the anomalies highs or lows, different from the measured magnetic anomaly map, where anomalies and their sources are out of phase.

After all the processing steps described in this section, the quality of the signal strongly improves (Figure 5). Most of the noise effects have been suppressed and, as expected, most of the anomalies have lost their dipolar shape, displaying a single high in correspondence to their sources.

The comparison between the maps of the total magnetic field (Figure 6) and of its vertical gradient (Figure 5(b)) demonstrates why the latter is usually preferred because of a higher information content and a better resolution power.

Many anomalies of the vertical gradient seem to be potentially related to archaeological sources (Figure 7). Linear patterns of anomalies extend for some tens of metres and a possible correlation with elongated structures of archaeological interest, like walls alignments or moats, could be hypothesized (red dashed lines in Figure 7). The presence of anomalies crossing each other in roughly perpendicular directions outlines patterns with such a geometric regularity that could be associated with the remains of dwellings. However, several high-amplitude anomalies (white dashed circles in Figure 7) still exhibit a dipolar shape, some of them with an orientation of the high-low axis suggesting a significant difference between the direction of magnetization and that of the present inducing geomagnetic field in the area. This might imply the presence of sources with a strong component of remanent magnetization, as often happens for several fired objects of archaeological interest (e.g. kilns, pottery, metal handicrafts, slag).

2 | DATA INTERPRETATION

2.1 | Methods

The interpretation of the data of vertical gradient of the total field followed two main lines: a description of the horizontal position of the anomaly sources and a quantitative estimation of their depths and general shape. More information about the data processing and
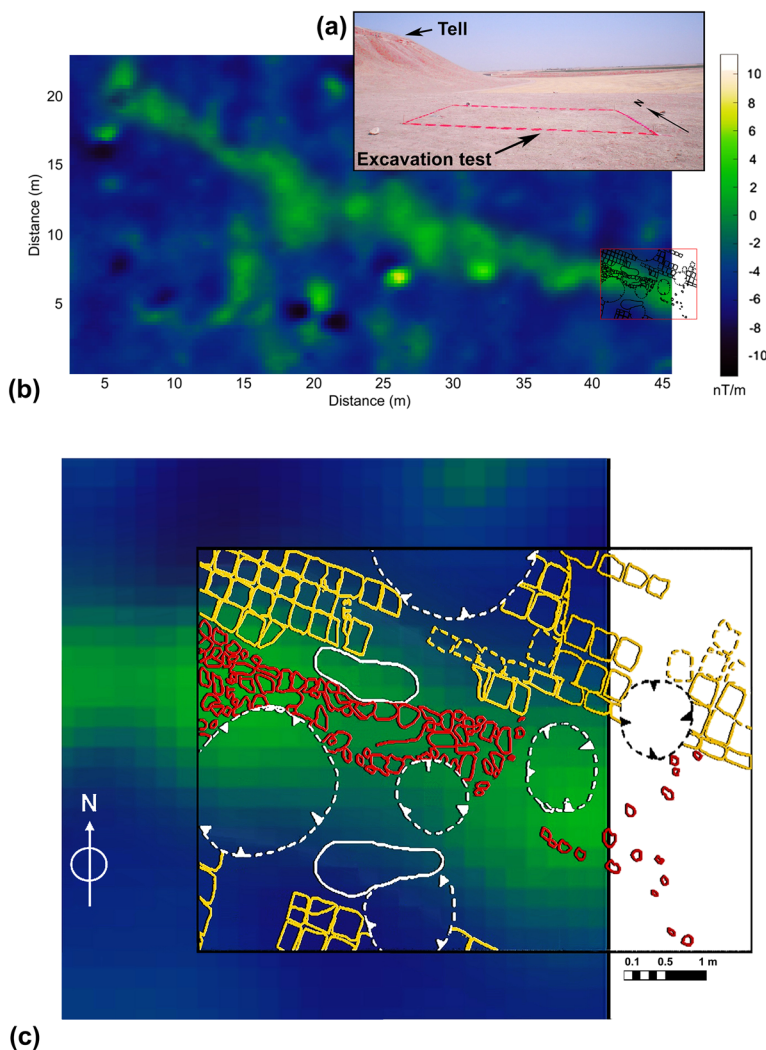
FIGURE 10 Excavation results in Area 1 (for the location, see Figure 7). (a) Photograph showing the location of the excavation test area (red rectangle) southeast of the tell (photograph© 'Archivio della Missione Archeologica Italiana a Tell Barri', 2010); (b) position of the excavation test area (red rectangle) with respect to the anomaly in Figure 9(a); (c) main results of the archeological excavation (drawing© 'Archivio della Missione Archeologica Italiana a Tell Barri', 2010, redrawn from original). Red texture: road paved with high susceptibility baked clay brick fragments; yellow texture: walls made of mud bricks; white and black dashed circles: buried pits [Colour figure can be viewed at wileyonlinelibrary.com]

interpretation methods used in the data analysis and interpretation can be found in the Appendix A, where examples of their application on simple synthetic magnetic fields are given, along with an explanation of their meaning and some operative details.

To have a clearer representation of the vertical gradient anomalies, some sort of smoothing may be useful. At the same time, a smoothing process may have the effect of reducing our ability to distinguish nearby anomalies, hindering a detailed identification of archeological structures. Thus, we define a processing sequence (smoothing–enhancing–filtering) that achieves the objective of obtaining a smooth yet informative magnetic map. We apply this operator to the reduced to the pole vertical gradient map (Figure 7) so that the effect of the bipolarity of the anomalies is decreased and the vertical gradient anomalies shift upon their source. Then, we upward continued (see Appendix A) the reduced to the pole anomalies to a higher elevation (e.g. Blakely, 1996) to reduce the noise and simplify the magnetic anomaly pattern. Finally, the upward continued field is vertically differentiated (see Appendix A) to enhance, and partially recover, the high wavenumbers content. This composite process leads to a band-pass filtering (Fedi, Florio, & Quarta, 2009), reducing both the lowest and highest wavenumbers from the original spectrum. It is important to emphasize that all the filters involved in this processing are physically based, so that we expect no arbitrary distortions of the original field as other purely mathematical filters may induce. To improve the recognition of the main vertical gradient trends, we apply for the first time in an archeological case the signum transform (Weihermann, Ferreira, Oliveira, Cury, & de Souza, 2018). This simple transformation, when applied to a second-order vertical gradient of a magnetic field (i.e. the field transformed according to the earlier described

processing), produces a binary image having a value of 1 over the sources and of −1 elsewhere (assuming that all the magnetic sources are generated by a positive magnetization contrast).

A further and final step of the interpretation is aimed at a better characterization of the most significant anomalies with possible archaeological meaning. To do this, we analysed the anomalies of the vertical gradient of the magnetic field (Figure 7) by using a multi-scale approach, based on the simultaneous analysis of the data computed at many altitudes above the measurement plane (DEXP – depth from extreme points, Fedi, 2007). To build this dataset, DEXP method uses again the upward continuation and the vertical differentiation of the input field (see Appendix A). It includes the analysis of the so-called scaling function, which depends on a parameter roughly characterizing the shape of the anomaly source, the structural index (N). Thus, DEXP provides important information about the anomaly sources, namely their depth and a simplified geometrical type (point, line, ribbon, 'contact'). DEXP is an effective 3D imaging method and seems very practical to model magnetic anomalies related to archaeological remains hidden below the ground level (Cella & Fedi, 2015; Cella, Paoletti, Florio, & Fedi, 2015).

3 | RESULTS AND DISCUSSION

The maps produced by our smoothing–enhancing operator allow for an easy description of the main magnetic trends. In Figure 8(a), we show the second-order vertical gradient of the reduced to the pole magnetic field upward continued to 1.5 m above the measurement surface. The image of Figure 8(a) is obtained using a histogram
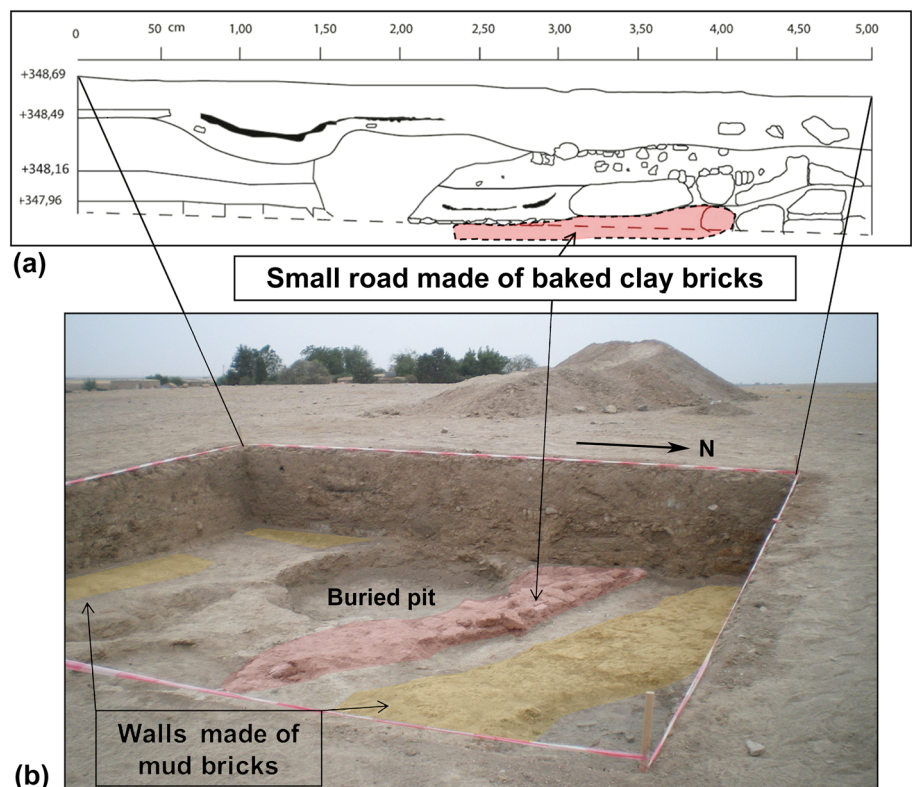
FIGURE 11 Excavation results in Area 1 (for the location, see Figure 7). (a) Stratigraphic section along the western edge of the excavation test area (located in Figure 10). Red colour indicates the presence of linear archaeological feature made of baked clay brick fragments; (b) photograph of the archeological excavation. Red and yellow colours represent the linear feature made of fired bricks, and walls made of mud bricks, respectively (photograph and drawing© 'Archivio della Missione Archeologica Italiana a Tell Barri', 2010) [Colour figure can be viewed at wileyonlinelibrary.com]

equalization algorithm, producing a non-linear colour scale, so that the amplitudes appear rather homogeneous even if a few dipolar anomalies have an amplitude much stronger than the average value. In Figure 8, we highlight the main linear anomaly trends with letters (if they are oriented roughly in a south–north direction) or numbers (when roughly oriented in a west–east direction). These trends are more clearly visible in the signum transform map (Figure 8(b)). At least six main south–north and four west–east linear anomaly trends, elongated for 20 to 30 m or more, can be identified. Many of them can be recognized as generated by coalescence of smaller anomalies, sometimes having a rectangular shape. This situation is very clear for anomaly b in Figure 8, both in its southern and northern parts (they are separated by a magnetic low at y = 30 m). In other cases, the elongated anomalies have a different character, being thinner and more regular in shape, as is the case of anomaly 4, in the northeast part of the map. In general, the south–north trends are rather regularly spaced, being separated by about 15 m (anomalies from b through f) and a similar distance separates west–east trends such as 2, 1 and 5, in the western part of the map. This rather regular sequence of alignments of anomalies may be interpretable with the possible presence of an urban network of streets and houses. The area enclosed between anomalies a and b and between anomalies 2 and 5 (Figure 8) represents well this situation and will be studied in detail later.

Given the large number of anomalies of the vertical gradient having interesting features, we will show here our analysis on some of the most promising areas from an archaeological point of view.

3.1 | Area 1

Among the most noticeable patterns of the vertical magnetic gradient, a linear anomaly stands out toward the north-eastern edge of the surveyed area (Area 1 in Figure 7; anomaly 4 in Figure 8), trending in a
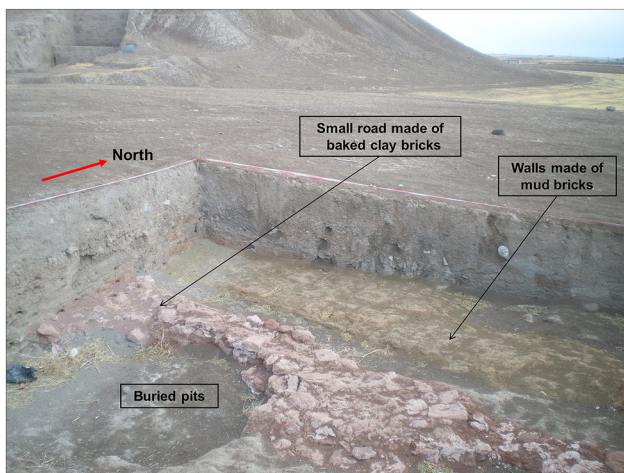

FIGURE 12 Excavation results in Area 1 (for the location, see Figure 7). Photograph of the archeological excavation. Red and yellow colours represent the small road made of baked clay bricks; and walls made of mud bricks, respectively (photograph© 'Archivio della Missione Archeologica Italiana a Tell Barri', 2010) [Colour figure can be viewed at wileyonlinelibrary.com]

west-northwest direction for at least 25 m (Figure 9(a)). The characteristics of such an anomaly are compatible with a linear buried structure possibly a stone-paved street, a moat, etc. To gain information about the burial depth and about the shape of the source we apply DEXP method in an area enclosing this anomaly. The analysis allowed estimating a structural index of about 1.75, indicating a source similar to a narrow horizontal ribbon-like body. Starting from this estimated value, DEXP analysis located the centre of the source at a depth of about 0.80 to 1.1 m below the ground level. We show the 3D position of the centre of the source as estimated by the DEXP method in Figure 9 (b), by using an iso-surface representation, indicating a longitudinal extent up to 25–30 m in the west-northwest–east-southeast

FIGURE 13 Data interpretation in Area 2 (for the location, see Figure 7). (a) Magnetic vertical gradient field, showing elongated anomalies interpretable as housing structures. The intense dipolar anomaly placed on its southwest side may be related to fired, highly magnetized materials (kilns, hearth steads, etc.) or to metallic objects; (b) iso-surface representation of the source imaging obtained by depth from extreme points (DEXP) method. The source centre is identified at a depth ranging from 0.3 m to 0.5 m below the ground level. The topography is indicated with red contours each 0.2 m. The magnetic vertical gradient is shown for reference in the background. The source may be interpreted as the structure of a small house dated tom the Parthian period [Colour figure can be viewed at wileyonlinelibrary.com]

direction. An archeological excavation was therefore planned based on this geophysical information. A square area of dimensions 6.75 m × 5 m (Figure 10(a)) at the eastern end of the linear source modelled by DEXP, was selected for the excavation (Figure 10(b)). The dig revealed the upper side of the linear architectural feature about 1 m large, elongating in the same direction as the vertical gradient magnetic anomaly, made of irregularly shaped baked clay bricks (Figures 11 and 12). The feature has a very good correspondence with the reduced to the pole magnetic anomaly (Figure 10(c)).

The stratigraphic section in Figure 11(a) shows that the linear feature was found at depths ranging from about 0.7 m to 1 m below the ground surface, in very good agreement with the depth estimated by DEXP method (Figure 11(b)). In addition, the whole shape of the source appears very similar to that indicated by the estimated structural index. These results let us hypothesize that the same structure continues for at least 15–20 m northwestward (Figure 9 (a)). However, the excavation revealed also the presence of other elements of archaeological interest (Figures 11b and 12), as several

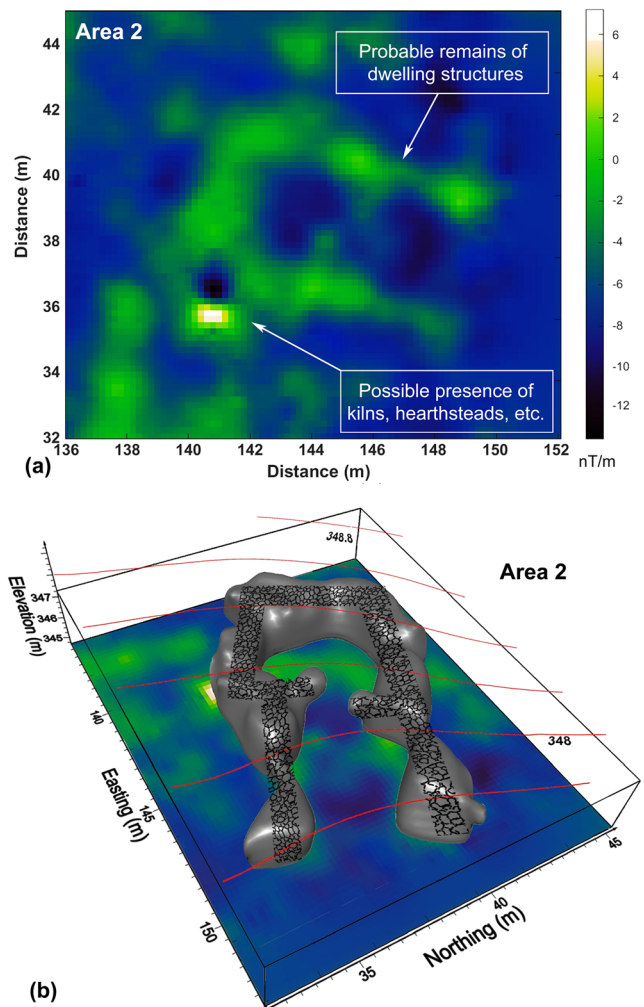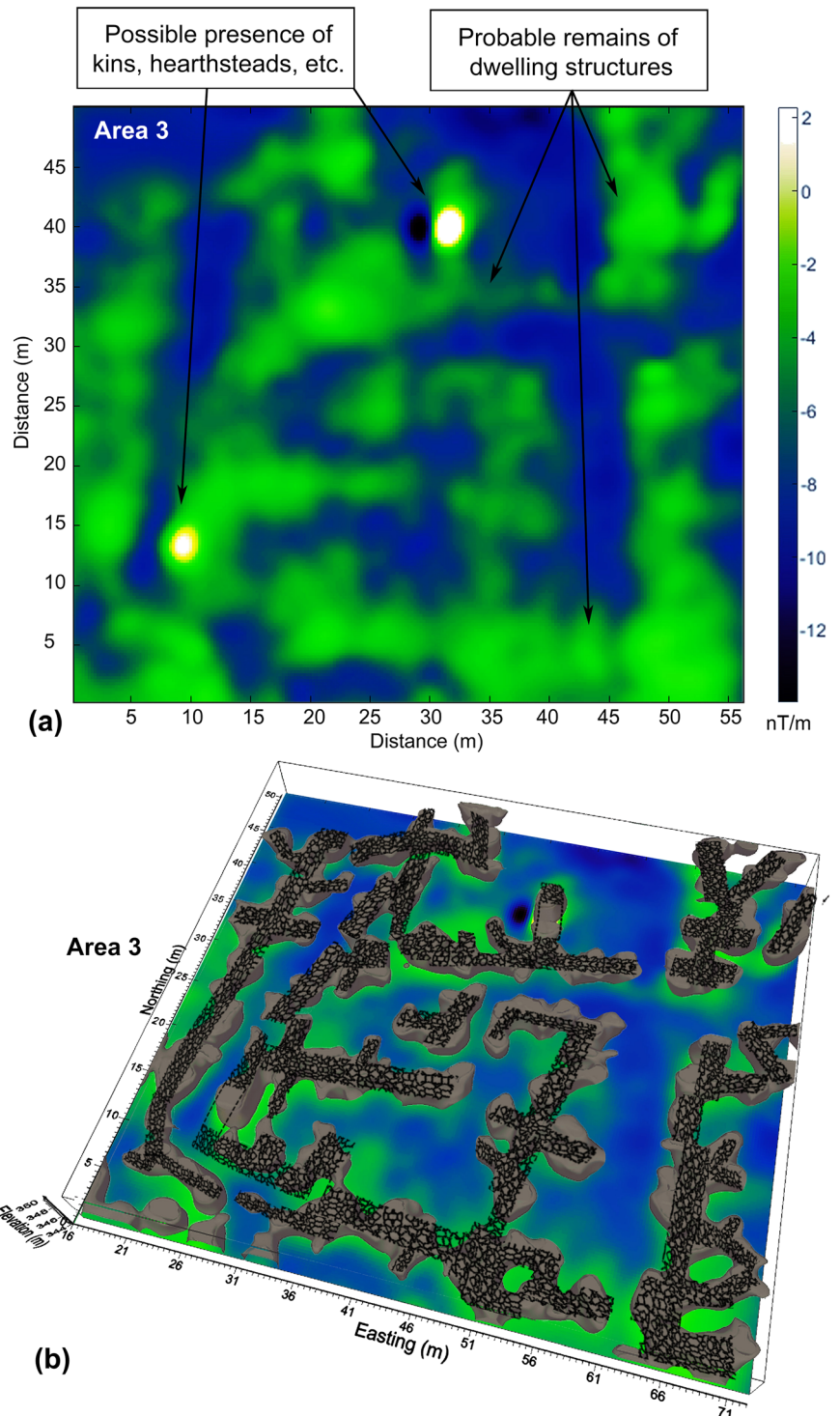**FIGURE 14** Data interpretation in Area 3 (for the location, see Figure 7). (a) Magnetic vertical gradient field, showing trends probably related to the plan of small urban network; (b) iso-surface representation of the source imaging obtained by depth from extreme points (DEXP) method. The source centre is identified at a depth ranging from 0.25 m to 1.5 m below the ground level. The magnetic vertical gradient is shown for reference in the background [Colour figure can be viewed at wileyonlinelibrary.com]

pits (evidence of later periods exploitation of the area) often destroying previous structures, and the remains of two walls of dwellings placed on both sides of the road and at the same depth (Figures 8(b) and 9). They are made by adobe bricks, and this explains the absence of any significant magnetic anomalies in correspondence of these structures.

3.2 | Area 2

Area 2 is located just south of the structure described in the previous section (Figure 7), where a small but well-defined pattern of anomalies is visible (Figure 13(a)). It is shaped like a rectangle open on its southeast side and with the longer sides northwest–southeast oriented.

By applying the same procedure followed for Area 1, the DEXP method was preceded by the analysis of the scaling function. A structural index $N \approx 2$, related to a linear shape of the source, was estimated. The 3D imaging of DEXP results revealed a roughly linear body, at a depth ranging from 0.3 m to 0.5 m below ground level, extended along the three sides of a 12 m × 7 m rectangle open on its south-eastern side and in which some internal arrangement seems visible.

It is highly probable that the modelled source (Figure 13(b)) is what remains of a wall of a small housing structure dated to the Parthian period. Interestingly, a high amplitude bipolar anomaly is present very close to the western corner of the anomaly pattern (Figure 13(a)). Such an anomaly is compatible with a highly magnetized source, like kilns, hearth steads, etc., that were usually built just outside the houses.

3.3 | Area 3

Finally, a third area was analysed in detail (Area 3 in Figure 7). Located in the south-western side of the survey, Area 3 is much larger than the two previously considered, extending for more than 50 m both in north–south and east–west directions.

The map of the vertical gradient of the magnetic field (Figure 14 (a)) shows a complex pattern of roughly linear anomalies. As already emphasized earlier, many of them can be recognized as generated by coalescence of smaller anomalies, sometimes having a rectangular shape. These anomalies have a rather regular geometry, visible despite the presence of local, high amplitude bipolar anomalies, related to the presence of shallow and strongly magnetized sources. This regular anomaly pattern can be considered as compatible with the presence of a small urban network of streets and architecture.

In this case, considering both the extension of the area and the complexity of the magnetic field, the application of the DEXP technique involved the analysis of the scale function in several points, representative of the different elements of the complete pattern of anomalies included in the map. We found structural index values falling in a range between ~1.5 and ~2.5, implying anomaly sources having a roughly linear shape. This value of the structural index was used to compute the DEXP transformation, returning the model shown in Figure 14(b). The 3D images point out the presence of several linear bodies lying along north–south and east–west directions and joined to each other, similarly to a small urban network, at a depth ranging from 0.25 m to 1.5 m below the ground level. Two strong amplitude bipolar anomalies may be interpreted as the magnetic expression of kilns or hearth steads.

4 | CONCLUSIONS

The geophysical survey at the lower town of Tell Barri proved very useful for hypothesizing the archeological potential of this vast area. The anomalies of the vertical gradient of the magnetic field depicts trends and structures likely corresponding to an urban network of roads and houses. The only one excavation located by the geophysical results done up to now, was successful in identifying a small road paved with fragments of baked bricks. We showed that to improve the S/N ratio of magnetic data it may be useful to make careful studies of the noise sources and a consequent arrangement of the magnetic gradiometer setting. In our case, a decreasing of the sensitivity of the system was needed to increase the S/N ratio.

In this article, we made a rather detailed study of several potentially interesting areas. However, many other interesting anomalies may have been interpreted throughout the surveyed area. This may be the object of further research. Unfortunately, in 2011, just after completion of the second survey, the Tell Barri region was ravaged by the bloody war events still continuing in Syria. This prevented further investigations in this important archeological area up today. However, the employment of methods used for magnetic 3D modelling of selected structures of archaeological interest demonstrated useful in the investigated area, thus confirming how techniques developed essentially for geological investigations can provide quite precious information also in the archaeological field studies, thus optimizing the costs/benefits ratio.

AUTHOR CONTRIBUTIONS

G. Florio supervised the project and contributed to data acquisition, modelling and interpretation. F. Cella contributed to data acquisition, interpretation and dealt with the 3D modelling and graphics. L. Speranza and R. Castaldo contributed to data acquisition and processing. R. Pierobon Benoit since 2006 is the Director of the archaeological exploration of Tell Barri, making possible to carry out the geophysical survey, and with R. Palermo provided data interpretation within the archaeological context of the site. All authors discussed the results and contributed to the final manuscript.

DECLARATION OF INTEREST

The authors have no a conflict of interest in relation to this work.

ORCID

Giovanni Florio 🅙 https://orcid.org/0000-0002-7841-2967
Federico Cella 🅙 https://orcid.org/0000-0001-5165-1709
Raffaele Castaldo 🅙 https://orcid.org/0000-0002-8425-0781

REFERENCES

Baranov, V. (1975). *Potential fields and their transformation in applied geophysics*. Stuttgart: Gebruder Borntraeger.

Blakely, R. J. (1996). *Potential theory in gravity and magnetic applications*. New York: Cambridge University Press.

Breiner, S. (1973). *Applications manual for portable magnetometers. S., California*. San José, CA: Geometrics.

Cella, F., & Fedi, M. (2015). High-resolution geophysical 3D imaging for archaeology by magnetic and EM data, the case of the Iron Age settlement of Torre Galli, southern Italy. *Surveys in Geophysics*, 36(6), 831–850. https://doi.org/10.1007/s10712-015-9341-3

Cella, F., Paoletti, V., Florio, G., & Fedi, M. (2015). Characterizing elements of urban planning in Magna Graecia using geophysical techniques: The case of Tirena (southern Italy). *Archaeological Prospection*, 22, 207–219. https://doi.org/10.1002/arp.1507

Ciminale, M., & Loddo, M. (2001). Aspects of magnetic data processing. *Archaeological Prospection*, 8, 239–246. https://doi.org/10.1002/arp.172

Fedi, M. (2007). DEXP: A fast method to determine the depth and the structural index of potential fields sources. *Geophysics*, 72(1), I1–I11. https://doi.org/10.1190/1.2399452

Fedi, M., Cella, F., Florio, G., La Manna, M., & Paoletti, V. (2017) Geomagnetometry for archeology. In N. Masini & F. Soldovieri (Eds.), *Sensing the past – From artifact to historical site*, 203–230. Springer, Berlin.

Fedi, M., & Florio, G. (2003). Decorrugation and removal of directional trends of magnetic fields by the wavelet transform: Application to archeological areas. *Geophysical Prospecting*, 51, 261–272. https://doi.org/10.1046/j.1365-2478.2003.00373.x

Fedi, M., Florio, G., & Quarta, T. (2009). Multiridge analysis of potential fields: Geometric method and reduced Euler deconvolution. *Geophysics*, 74(4), L53–L65. https://doi.org/10.1190/1.3142722

Fedi, M., & Quarta, T. (1998). Wavelet analysis for the regional-residual and local separation of potential field anomalies. *Geophysical Prospecting*, 46(5), 507–525. https://doi.org/10.1046/j.1365-2478.1998.00105.x

Florio, G., Fedi, M., & Pasteka, R. (2014). On the estimation of the structural index from low-pass filtered magnetic data. *Geophysics*, 79(6), J67–J80. https://doi.org/10.1190/GEO2013-0421.1

Florio, G., Fedi, M., & Rapolla, A. (2009). Interpretation of regional aeromagnetic data by the scaling function method: the case of Southern Apennines (Italy). *Geophysical Prospecting*, 57(4), 479–489.

Gaffney, C. (2008). Detecting trends in the prediction of the buried past: A review of geophysical techniques in archaeology. *Archaeometry*, 50, 313–336. https://doi.org/10.1111/j.1475-4754.2008.00388.x

Gibson, T. H. (1986). Magnetic prospection on prehistoric sites in western Canada. *Geophysics*, 51, 553–560. https://doi.org/10.1190/1.1442109

Ilaiwi, M. (1985). *Soil map of Syria and Lebanon*. Damascus: Arab Center for the Studies of Arid Zones and Dry Lands (ACSAD).

Larson, D. O., Lipo, C. P., & Ambos, E. L. (2003). Application of advanced geophysical methods and engineering principles in an emerging scientific archaeology. *First Break*, 21, 51–62.

Palermo, R. (2019). *On the edge of empires. North Mesopotamia during the Roman period*. London: Routledge. https://doi.org/10.4324/9781315648255

Paoletti, V., Fedi, M., Florio, G., & Rapolla, A. (2007). Localized cultural denoising of high-resolution aeromagnetic data. *Geophysical*

Prospecting, 55(3), 421–432. https://doi.org/10.1111/j.1365-2478.2007.00623.x

Pecorella, P. E. (1998). *Tell Barri/Kahat 2. Relazione sulle campagne 1980–1993 a tell Barri/Kahat, nel bacino del Habur (Siria)*. Rome: Documenta Asiana, CNR - Consiglio Nazionale delle Ricerche.

Pierobon Benoit, R. (2018). Tell Barri/Kahat 2000–2010: The contribution of the excavations to the history of the Jazira. In J. Abdul Massih, & S. Nishiyama (Eds.), *In collaboration with H. Charaf and A. deb* (pp. 145–153). Oxford: Proceedings of ISCACH-Beirut.

Pierobon Benoit R., & Pecorella, P.E. (2008) Tell Barri. Storia di un insediamento antico tra Oriente e Occidente. Pierobon Benoit R. Ed., «La Parola del Passato» 63, Macchiaroli, Napoli.

Tabbagh, J. (1999). Filtrage numérique des donnes géophysiques. In M. Pasquinucci, & F. Trément (Eds.), *Non-destructive techniques applied to landscape archaeology*. Oxford: Oxbow Books.

Weihermann, J. D., Ferreira, F. J. F., Oliveira, S. P., Cury, L. F., & de Souza, J. (2018) Magnetic interpretation of the Paranaguá Terrane, southern Brazil by signum transform. *Journal of Applied Geophysics*, 154, 116–127. http://doi.org/10.1016/j.jappgeo.2018.05.001.

APPENDIX A

Here we give some more detailed information about the magnetic data transformations used in the article (reduction to the pole, vertical differentiation and upward continuation) as well as the 3D interpretative method used (DEXP). While we refer to specific textbooks for a detailed mathematical description (e.g. Blakely, 1996; Hinze et al., 2013), here we want to highlight their practical utility in the analysis of magnetic data in archaeological contexts. Moreover, emphasis will be given to the operational details and on the interpretation of the results.

The magnetic data processing and modelling described in this article was done using software developed by the authors in Matlab environment. However, commercial implementations for the magnetic data transformations (e.g. Geosoft suite) or 3D display (e.g. Surfer, Voxler) are available.

DWT filtering

The word 'filtering' refers to those processes aimed at suppressing particular frequency bands within a signal. Filtering of geophysical data is an often-required processing step. In magnetic data processing, filtering may be needed to remove noise or reduce the effects of regional, long-wavelength fields. In any case, the process aims at enhancing the useful signal.

Commonly, this operation is performed in the wavenumber domain, multiplying the Fourier-domain transformed data by a suitably designed filter. The main weakness of Fourier analysis is that it cannot account for the local behaviour of a function, the filter acting in all the analysed area, i.e. there is no spatial resolution.

In recent years, another approach to filtering has been defined, based on the Discrete Wavelet Transform (DWT; Fedi & Quarta, 1998). While the Fourier analysis decomposes a signal in a series of infinitely long sinusoidal functions, DWT relies on functions ('wavelets') having the property of being localized in space. Thus, the main advantage is that the analysis is based on mathematical models characterized by both a frequency and a space resolution, so that a local filtering is possible. In practice, this filtering is based on a specific space-scale wavelet analysis, known as multiresolution analysis, allowing the decomposition of the signal in a pre-defined range of scales. Here the concept of scale is similar to that of frequency, where a large scale is associated to a large wavelength, and a small scale is associated to a small wavelength. The total signal is the sum of several 'details' at different scales, and each detail is defined with components in the x, y and diagonal directions.

Thus, this decomposition easily allows a localized and directional filtering (Fedi & Florio, 2003; Paoletti, Fedi, Florio, & Rapolla, 2007) to be performed. In this article, we used this approach to remove the striped noise localized in the direction of the survey lines (north–south). This result was obtained by zeroing the DWT coefficients related to the y direction at the two highest scales in all the survey area. The signal is then reconstructed using the modified DWT coefficients. As with any filtering process, the analysis of the residual signal (i.e. the original signal minus the filtered one) should make sure that no distortion of the anomaly trends is produced. In a directional filtering case, the residual map should contain only anomalies elongated in the filtering direction and uncorrelated with the useful signal.

In the case of the gradiometric data at Tell Barri, we chose the 'Interpolating' wavelet and the field was separated into nine components relative to different frequencies ('scales'). The stripe-shaped noise resulted well suppressed by reconstructing the field after zeroing the DWT coefficients related to the y direction at the two smallest scales (i.e. the eighth and ninth) in the whole area. The residual map relative to the directional filtering performed to 'decorrugate' the Tell Barri vertical gradient anomalies (Figure A1) demonstrates the correctness of the process. In the residual map, the only features having a correlation with possible archaeological anomalies are localized in correspondence to some high-amplitude anomalies that are not quantitatively interpreted in this article.

Reduction to the pole

At intermediate magnetic latitudes (i.e. when the magnetic field inclination varies from about 25° to 80°), the shape of a magnetic anomaly generated by an underground source magnetized by induction will have a clear bipolar structure, with a magnetic field high toward the equator and a magnetic low, toward the geographic pole (this description is valid both in the Northern and the Southern Hemispheres, for a positive magnetization contrast). Unfortunately, the source position will be in between the position of the magnetic high and low, so that it cannot be easily determined by a simple inspection of a magnetic map. On the contrary, in polar areas (magnetic field inclination > 80°) the field is subvertical and the magnetic anomalies are characterized essentially by a single magnetic high positioned above the sources, while in equatorial areas the field is nearly horizontal and the resulting anomaly has a main low in correspondence to the source position. The reduction to the pole aims at transforming the measured magnetic anomalies at intermediate latitudes to those that would have been measured at the magnetic pole, in the case of a purely induced magnetization. Therefore, the analysis of the RTP map allows accurate positioning of the magnetic sources, which will be located in correspondence to the magnetic highs (for positive magnetization contrasts; Figure A2).

This transformation is performed in the wavenumber domain by multiplication of the Fourier transform of the data by a specific filter. The reduced to the pole magnetic data are then obtained by anti-
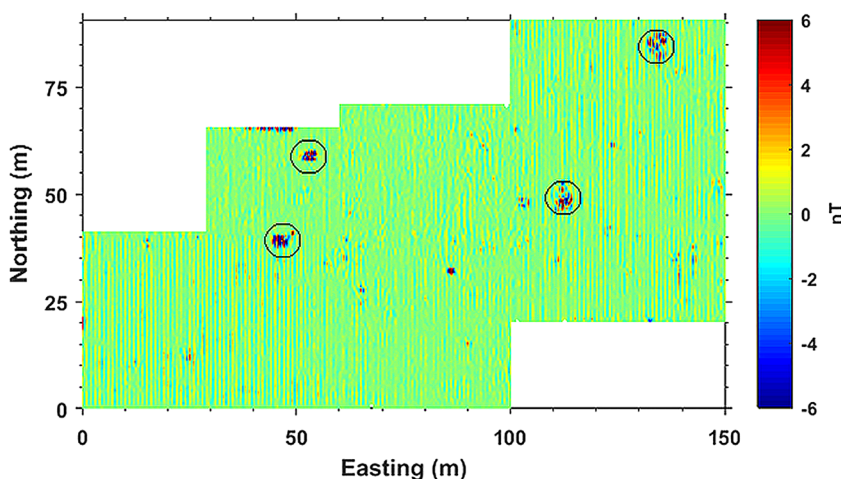

FIGURE A1 Tell Barri magnetic survey: 'residual' map obtained by subtracting the DWT directional filtered data and the original ones. As expected, the resulting anomalies are elongated in the filtering direction and generally uncorrelated with the useful signal, except in correspondence to some high-amplitude anomalies not quantitatively interpreted in this article (black circles) [Colour figure can be viewed at wileyonlinelibrary.com]

FIGURE A2 (a) Synthetic magnetic anomaly generated by two prismatic sources, having a 50° inclination and 30° declination for both the inducing field and magnetization vectors. (b) Anomalies in (a) reduced to the pole. Differently from (a), in (b) the sources' position corresponds well to the magnetic highs [Colour figure can be viewed at wileyonlinelibrary.com]
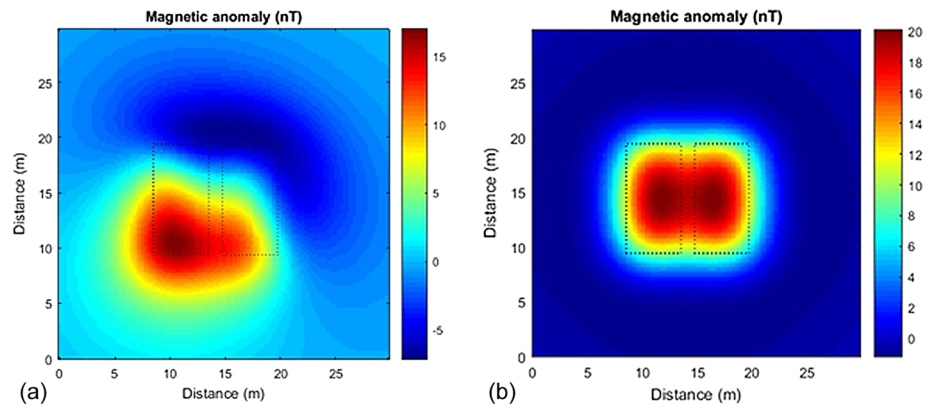
transforming the result. The input parameters for the filter definition are: (1) the direction (i.e. inclination and declination angles) of the Earth's magnetic field at the survey time and location, as given by the International Geomagnetic Reference Field (IGRF) model (available at many scientific institutions web resources, e.g. https://geomag.nrcan.gc.ca/calc/mfcal-en.php) and (2) a guess about the direction of the source total magnetization vector (which is unknown). Generally, the magnetization can be considered as purely induced by the Earth's magnetic field, so that the same direction of the IGRF can be assumed. If this assumption is approximately valid, the resulting anomaly will display a symmetric shape, with the position of the main magnetic high now slightly shifted toward the magnetic pole with respect to the original anomaly and corresponding to the source position (Figure A2). On the contrary, if the source has a strong remanent magnetization (as happens in metallic objects, baked bricks, etc.) oriented in a direction different from that of the IGRF, the transformed anomaly will be distorted, maintaining a deep magnetic low. Thus, the nature of the sources can also be investigated by the inspection of the transformed map.

Upward continuation

Magnetic maps, especially vertical gradient ones, can be characterized by the diffuse presence of small wavelength anomalies that disturb a

qualitative analysis and any quantitative interpretational steps. This noise can be attenuated or removed by the application of mathematical filter procedures, but this type of filtering can be too subjective, and the results could disrupt the anomaly integrity.

A very good alternative is the use of the upward continuation filter. From the potential theory, there is the possibility to compute the magnetic field that would be measured at an altitude higher than the measuring one, starting from the original data. The magnetic field attenuates with an increasing source-observation distance, but this attenuation is not equal at all the wavenumbers: great wavenumbers, corresponding to small wavelengths and related for example to small and shallow sources ('noise'), attenuate faster than small wavenumbers. This means that an upward continued map will be smoother than original data (Figure A3).

This transformation is generally performed in the wavenumber domain by multiplying the Fourier transform of the original data by a filter represented by a negative exponential function of the wavenumbers, where the exponent includes the elevation difference between the original and computation altitudes (the greater this difference, the smoother the resulting map). Thus, the only parameter needed is the continuation altitude, which can be chosen after some trials.

A mathematical lowpass filter and the upward continuation are both smoothing filters. However, the upward continuation is physically sound, meaning that the result will always represent a physically

FIGURE A3 (a) Synthetic magnetic anomaly generated by two prismatic sources, for a vertical inclination of both the inducing field and magnetization vectors. Notice the small wavelength noise added to simulate the effect of small and shallow sources or measurement errors. (b) Upward continuation of the data in (a) to an altitude above the measurement surface corresponding to three times the map sampling step (0.75 m). The noise is removed, and the magnetic field is smoother than the original field (a) [Colour figure can be viewed at wileyonlinelibrary.com]
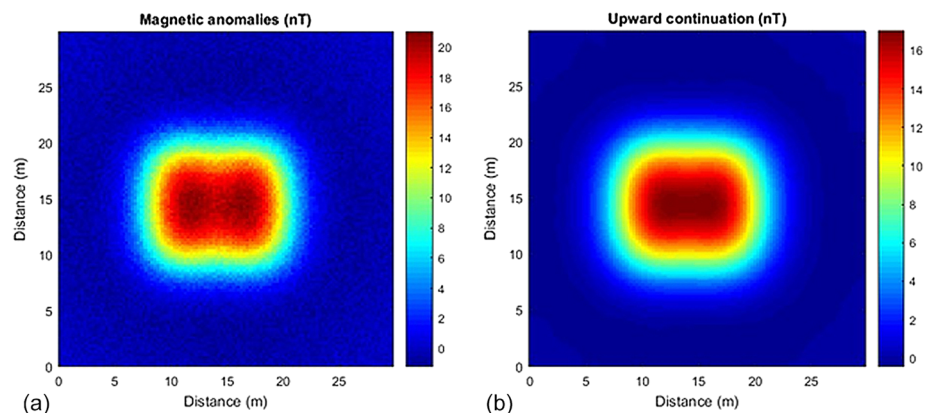
good result, contrarily to the output of a mathematical filter that may badly distort the original field (e.g., Florio, Fedi, & Pasteka, 2014).

Vertical differentiation

The vertical differentiation is another wavenumber domain transformation of the magnetic field. It computes a vertical gradient of the data without the need of a physical measure of the field at two locations (as is routinely done in surveys with magnetic gradiometers). Again, this possibility is theoretically granted by the potential fields' theory, so this transformation (just as upward continuation) is physically sound. The input parameter is simply an integer representing the differentiation order. In a vertically differentiated map, all the small wavelengths will be enhanced (i.e. it acts similarly to a high-pass filter), while a constant field is removed and slowly varying 'regional' fields are comparatively attenuated. The transformed magnetic field shows an increase of the resolving power, allowing a better separation of the anomalies generated by sources close to each other (Figure A4). This increase of 'resolution' can also have the drawback of disrupting the lateral continuity of elongated anomalies into several single, isolated anomalies.

In the present article, an interesting use of this transformation is presented, consisting in combining the vertical differentiation with upward continuation to build up a composite operator acting as a band-pass filter ('smoothing–enhancing' operator, Figure 6(a)): the resulting map will enjoy the smoothing properties of an upward continued map but thanks to the differentiation, without the typical resolution loss (Figure A5).

Depth from extreme points (DEXP)

The DEXP (Fedi, 2007) is a 3D source imaging tool for magnetic data. It uses a 3D dataset, built with the measured data and their upward continued version to a set of altitudes. To improve resolution, the dataset can consist of n-order vertical-differentiated data at a set of altitudes (where n stands for the differentiation order; see previous section). This 'multiscale' approach, where data at different altitudes are simultaneously used in the modelling, allows the depth to magnetic sources with only a limited amount of a priori information to be determined.

The DEXP transformation is computed by simply multiplying the 3D dataset by a power law of the altitude, where a parameter defining the source geometry is included in the exponent. The field scaled this way will display extreme points (highs or lows) at an altitude, z, corresponding to the depth, $-z$, of a characteristic point of a set of simple equivalent sources (point, line, sheet, half space or 'contact'). The geometry of the source is characterized by a structural index, which can be estimated by a study of the so-called 'scaling function' (Fedi, 2007; Florio, Fedi, & Rapolla, 2009), defined as the ratio between the logarithm of the data and the logarithm of the respective altitude. Details on this computation are explained in Florio, Fedi et al. (2009).

The application of this analysis results in a 3D volume of the rescaled field, where the meaningful points are relative to its extrema (Figure A6). A possible representation involves the creation of iso-surfaces by a graphical software, to obtain a 3D visualization around a maximum, representing an approximation to the true source volume (e.g. Figures 7, 11 and 12).
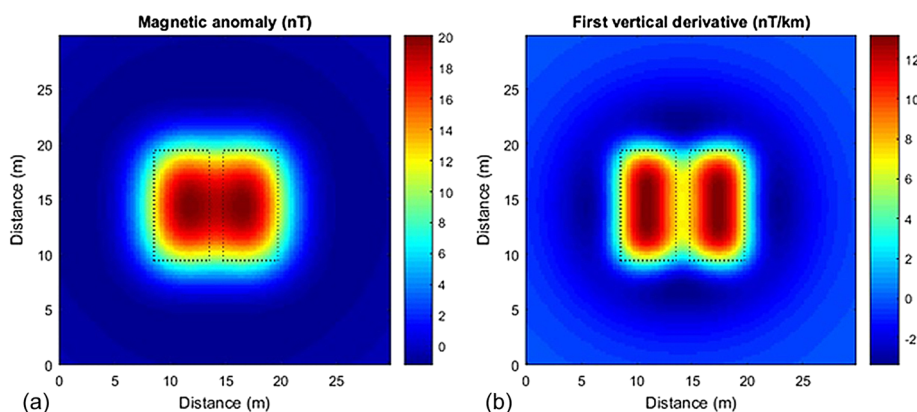

FIGURE A4 (a) Magnetic anomaly generated by two prismatic sources (outlined by the dotted lines) for a vertical inclination of both the inducing field and magnetization vectors. (b) First vertical derivative of the field in (a). Differently from (a), the map in (b) clearly shows the presence of two distinct magnetized sources [Colour figure can be viewed at wileyonlinelibrary.com]

FIGURE A5 (a) First vertical derivative of the noisy magnetic anomalies in Figure A2(a). Notice the strong enhancement of the noise. (b) Upward continuation of (a) to an altitude above the measurement surface corresponding to three times the map sampling step (0.75 m). The upward continuation effectively smooths the noisy original field, while the vertical differentiation recovers part of the lost resolution (smoothing/enhancing filter) [Colour figure can be viewed at wileyonlinelibrary.com]
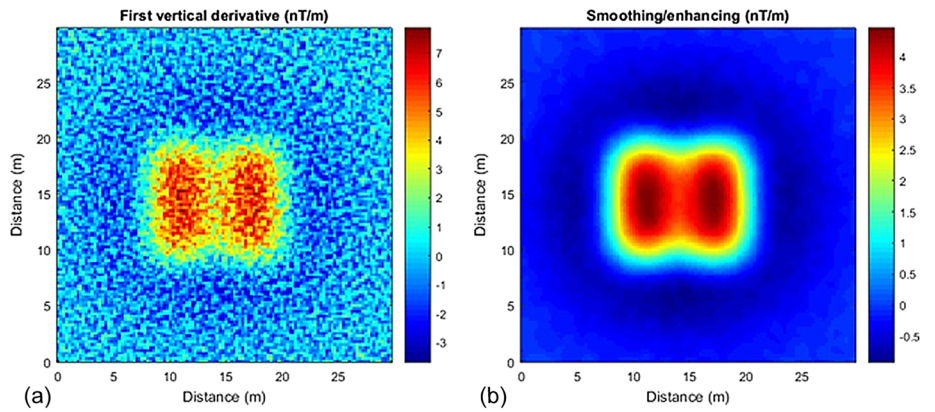

FIGURE A6 Example of depth from extreme points (DEXP) imaging (from Baniamerian et al., 2016). (a) Synthetic gravity anomalies generated by two prismatic sources (white rectangles in b) at the ground level. (b) DEXP image: the maxima of the rescaled field correspond to the sources' location. Notice that in (b) the vertical axis corresponds to the negative of the data altitude [Colour figure can be viewed at wileyonlinelibrary.com]